This is a preprint. Please check (and cite ☺) the accepted version at:

Polymer

Volume 173, 31 May 2019, Pages 20-26

DOI: 10.1016/j.polymer.2019.04.016

https://doi.org/10.1016/j.polymer.2019.04.016

The SI is attached at the end of this file.

SI videos are available at:

https://hagayshpaisman.wixsite.com/shpaismanlab/copy-of-videos

Simultaneous Polymerization and Patterning: A One Step Acoustic Directed Assembly Method

*Silvia Piperno, Haim Sazan and Hagay Shpaisman**

Department of Chemistry, Institute for Nanotechnology and Advanced Materials, Bar Ilan University, Ramat Gan, 5290002, Israel

ABSTRACT: Processing materials to form microstructures in the least possible number of steps is desired in order to reduce cost and processing time. In this work, we propose a new approach where standing surface acoustic waves are used to order materials prepared *in-situ* rather than preformed materials, providing a new method for one-step (simultaneous polymerization and patterning) directed assembly. We demonstrate this concept on products of an ongoing chemical reaction such as polymerization of polydimethylsiloxane (PDMS). We have found that by directed coalescence of nano-sized intermediate nucleation sites, continuous polymeric microstructures

are formed. A systematic study of the parameters that control this directed coalescence (cross-linker ratio, salt concentration and acoustic field strength) was performed. Acoustic forces can influence almost all dispersed systems, require low power densities and can be scaled up. Combining chemical synthesis with the patterning processes as shown here, could therefore be beneficial for directed assembly of soft matter.

KEYWORDS*:* Soft Matter, Directed Assembly, Coalescence, Colloids, Acoustic Manipulation

Introduction:

A chemical reaction is a well-determined process that converts one set of chemical compounds to another. The initial substances and environmental conditions determine the final product's nanoscopic and mesoscopic properties. Numerous chemical procedures have been developed to produce nanostructures and microstructures but achieving on-demand patterns is still challenging. Two main approaches have been developed to obtain desired patterns: Top-down and bottom-up [1]**.** The top-down approach (such as photolithography, soft lithography[2] or laser-ablation techniques) requires several steps to form the desired patterns, and is characterized by considerable waste of material. Some bottom-up techniques (such as ink-jet [3]or photo-thermal [4] printing) require the synthesis of nanomaterials that are then directed to form microstructures, while other methods (self-assembly and directed assembly) [1,5–9] are restricted to particular types of materials with specific physical or chemical properties. Methods that apply external physical forces on materials to govern the chemical reactions (such as electric fields, mechanical vibrations, oscillatory shear and temperature [10–13]) were not used for spatial control over the products, and therefore cannot be considered bottom-up approaches. The ability to process various materials to form microstructures in the least possible number of steps is an important issue in many fields such as electronics, sensing and biology. Recently, we have demonstrated how external forces such as optical traps can be used to influence ongoing chemical reactions and control colloid formation [14]**.** This represents an important step forward, but this technique requires a high amount of energy per area and is limited in its choice of material due to the required optical properties. Using acoustic forces as an alternative can pave the way towards one-step directed assembly. Acoustic manipulation is a powerful technique for assembly of particles. A suspended particle subjected to an ultrasound standing-wave field responds to the primary acoustic radiation force [15,16] by migrating to defined locations along the wave (pressure nodes or anti-nodes). Among manipulation techniques such as electric [5,17], optical [6,18], optoelectronic [7] and magnetic tweezers [8], acoustic techniques have a significant advantage, as their only requirement is a difference in compressibility and density between the particles and surrounding medium (acoustic contrast), which is true for almost all dispersed systems. The power density required to manipulate particles with acoustic forces is also several orders of magnitude smaller than that of its optical counterparts [16] and can influence a much larger area. Recently, standing surface acoustic waves (SSAWs) were used to manipulate and sort biological cells and particles in 2D [16,19] and 3D [20], study cell-cell interactions [21], to enrich cells [22] and protein crystals [23], to selectively promote coalescence [24,25] and to create ordered colloidal crystals [26]. In this work, we propose a new approach where SSAWs are used to deposit in predetermined locations the products of ongoing chemical reactions such as PDMS polymerization, providing well-

ordered and continuous polymeric microstructures in a single step. Previous works have shown localization of separate objects [26,27] and formation of permanent microstructures only with preformed materials [25,28]. This is the first realization of SSAWs being used to manipulate materials formed in-situ. Polymerization of PDMS was chosen because it is a well-known process [29,30] that is biocompatible and has many useful applications [31]. Additionally, the amount of cross-linker in this system can easily be changed by varying the ratio between the di-functional and tri-functional components, dimethyldiethoxysilane (DMDES) and methyltriethoxysilane (MTES, serves as the cross-linker), respectively. This gives an important handle on microstructure formation.

Experimental Methods:

Device fabrication: Standing surface acoustic waves were obtained on the surface of a lithium niobate single-crystal, 128° Y-rotated, X-propagating 3-inch wafer. Both double-sided and single-sided polished crystals were used with no apparent differences. A pair of interdigital transducers (IDTs) were fabricated on the surface of the wafer using standard soft photolithography procedures. A layer of a photoresist (1µm AZ 5214 E, microchem) was spin coated, irradiated by a UV light source through a photo-mask and, was subsequently, developed in a photoresist developer (AZ 351B, microchem). A double metal layer of 5nm adhesion layer of chromium and 100nm gold was evaporated by an electron beam evaporator and a lift-off process was used to remove the photoresist. The SAW's wavelength is defined as $\lambda = v/(f)$ where the acoustic velocity in lithium niobate (X-propagating) is v= 3997 ms^{-1} and f is the frequency of the applied signal. Measurements were performed on two devices: (I) 25 finger electrode pairs with 120 µm finger pitch operating at 32.8 MHz (Fig. 1) and (II) 40 finger electrode pairs with 200 µm finger pitch operating at 19.4 MHz (Fig. 2-5). The mark space ratio of each IDT finger array is 1:1, while acoustic aperture of each device is 1.9 mm. The radio frequency signal was generated by a dual channel arbitrary function generator (Siglent SDG 5162). The applied voltage to each IDT in all experiments was held constant at peak-to-peak amplitude of 20 V_{pp} (resulting in a force of $3.3*10^{-13}$N on 1µm sized PDMS spheres, see supplementary information).

Microfluidic channel fabrication: The PDMS microchannels (22 µm height) were fabricated by standard soft lithography and mold replica procedures. The photoresist (AR-N-4400-50) was spin-coated on a silicon- wafer substrate and developed with a photoresist developer (AR400-44). The silicon mold was coated with 1,1,1,3,3,3, hexamethyldisilizan (Merck). Sylgard TM184 silicon elastomer base and SylgardTM184 silicon elastomer curing agent (Dow Corning) were mixed in a 10:1 weight ratio, cast on the silicone mold, outgassed and cured at 80ºC for 2 hours. Finally, they were peeled off the silicone mold.

Surface treatments: A glass cover slip (160 µm thick) was used as a substrate for the PDMS line pattern deposition. The glass cover slip (18X9 mm) was bonded to the PDMS to form the micro channel. The micro channel was then positioned between the two IDTs. In order to activate the bounding surface of PDMS and to avoid deposition of emulsion drops on the PDMS microchannel, UV Ozone treatment was performed only to the PDMS channel. Silicon oil (IMMOIL-F30CC, Olympus) was used to acoustically couple the glass substrate to the lithium niobate chip. The oil also partially covers the IDTs (see Fig. S1 in SI).

Sample preparation: 0.6 ml of ammonia 25% (Carlo Erba) was added to 1.9 ml of DI water. A mixed solution of Dimethyldiethoxysilane (DMDES, Acros Organics) and trimethoxysilane (MTES, Alfa Aesar) was added, resulting in a solution where the monomers are 12.5 wt%. Cross-linker ratio is defined as wt% of MTES from the total monomer weight. For each set of parameters, at least 5 samples were prepared and measured. Na_2SO_4 (Stream Chemicals) was added (0.7 wt%, unless stated otherwise) to screen charges. The solution was shaken vigorously with a Vortex. Without activation of the acoustic waves, homogenous spherical PDMS colloids are formed (see video SV4. For 80% cross-linked PDMS, spheres stabilize at a dimeter of 1.1±0.2μm) [32]**.**

Characterization methods: Bright-field microscopy images were acquired (through the top of the PDMS micro-channel) by a Nikon Eclipse LV100ND microscope equipped with Nikon objective lenses: 5X (MUE120500), 10X (MUE 21200) and 20X (MUE 21500). A CMOS camera (Deltapix HDMI16MDPX, 1/2.8" sensor) was used to acquire images with a resolution of 0.15 μm/pixel for the 20X objective lens. SEM images were obtained using a Quanta FEG 250 System (HV 5-15KV). The height and width of the line measurements were obtained by using a profilometer (Veeco Dektak 150 system; Stylus radius 12.5μm, Force 0.5mg; Resolution 0.074 μm/sample).

Result and discussion:

A pair of interdigital transducers (IDTs) is deposited on a transparent piezoelectric substrate (lithium niobate). Once a radio frequency (RF), is applied to both IDTs, two series of surface acoustic waves propagate in opposite directions and their superposition results in the

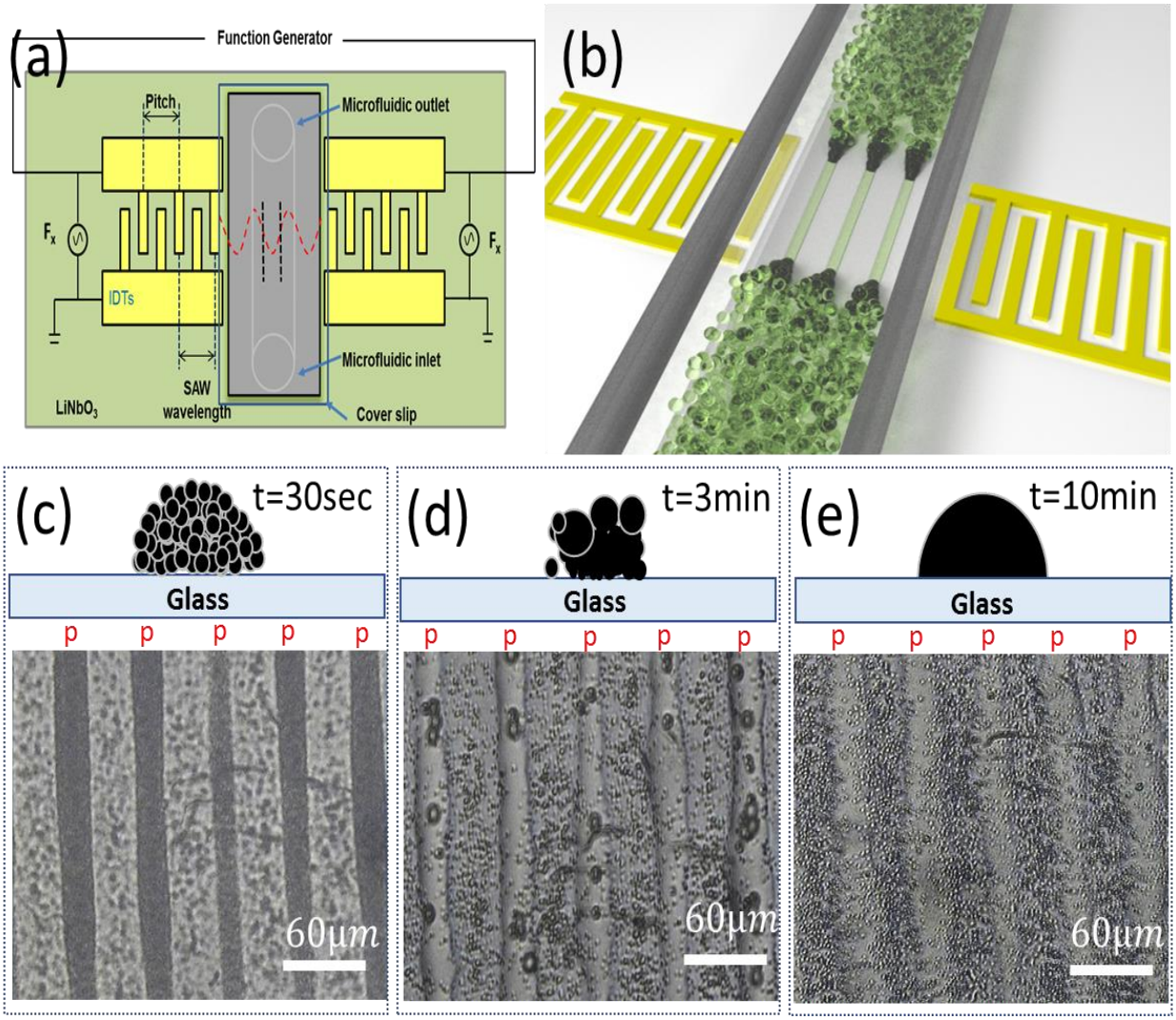

Fig. 1 a,b) Illustration of polymeric microstructure formation from a solution undergoing polymerization while applying SSAWs. In a) the red dashed line represents the standing acoustic wave and the black dashed lines represent the acoustic pressure node areas where the nucleation sites are directed. Fig.s 1c-1e show the assembly over time (in-situ bright field microscopy images, and illustration of a cross-section of a single line) at F=32.8 Mhz. c) 30 seconds after turning on the SSAWs. d) After 3 minutes, particles coalesce forming continuous lines. e) After 10 minutes, droplets have fully merged. The letter "p" in red is shown above the location of the PDMS lines.

formation of a SSAW[16]. The emulsion undergoing polymerization is infused into a PDMS microfluidic channel that is bonded on a glass cover slip [33] and positioned between two IDTs (Fig. 1a, 1b and S1 in SI). Silicon oil was used to acoustically couple the glass substrate to the lithium niobate chip.

The SSAWs direct nucleation sites to the position of the pressure nodes. Once two or more of these moieties are trapped, the acoustic force causes them to coalesce, eventually forming polymeric microstructures (Fig. 1b). The process can be divided into two main steps:

1) The nucleation sites are directed to node positions and coalesce (minimizing surface tension) to larger spherical micron-sized droplets.

2) The droplets wet the glass surface along the pressure nodes and merge due to the acoustic force leading to formation of continuous micro-structures. These steps are shown in Fig. 1c-1e.

The fixed parameters throughout the manuscript (unless stated otherwise) are: 20Vpp signal at a frequency of 19.4MHz, 12.5 wt% emulsion solution with 80% cross-linker and 0.7 wt% sodium sulfate.

After ~10 minutes from the time of solution preparation, sub-micron nucleation sites become visible inside the microchannel using bright-field microscopy. Once the SSAWs are generated, patterns appear within less than 30 seconds (Fig. 1c and Videos SV1 and SV2). The nucleation sites and droplets continue to accumulate until, after 3 additional minutes, they merge to form a continuous microstructure that is permanently attached to the bottom surface (Fig. 1d). Only a few droplets are positioned along the polymerized lines that have not yet merged. After 7 additional minutes, the droplets along the nodes have fully merged (Fig. 1e). A sequence of images showing a zoom in of the coalescence and merging process is presented in Fig. 2a-e and Video SV3. In the video, coalescence and merging of individual droplets are clearly visible. Fig. 2f shows a wide view (~1.0X1.8 mm) of the formed lines, 9 minutes after infusion. The formed structures

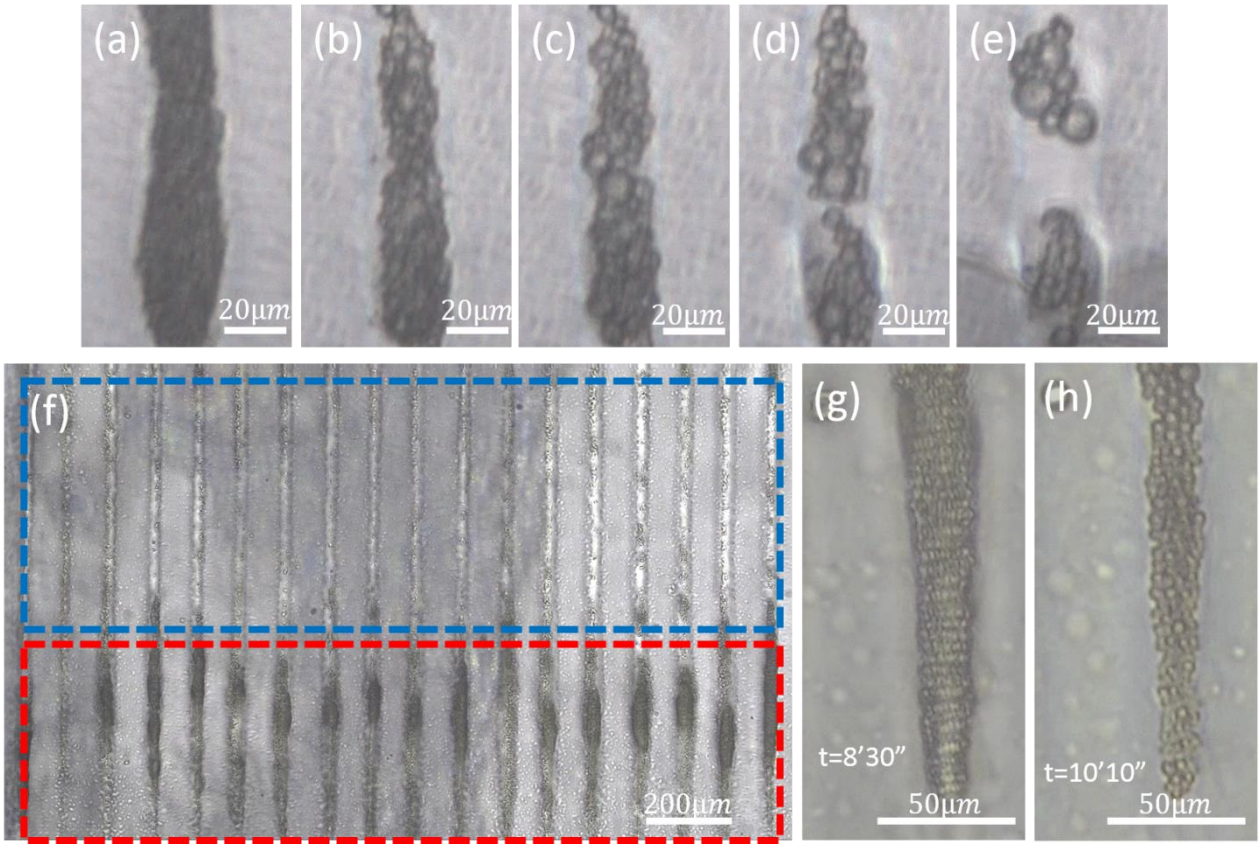

Fig. 2 Bright field microscopy images (in situ). a-e) Images of the coalescence process at: a) 4'54" b) 7'18" c) 7'38" d) 7'58" e) 8'18". See also Video SV3. f) Wide view of almost the entire width of the PDMS microchannel (~1.8mm showing 18 lines), after 9 minutes. There are two distinct regions: a region where almost all droplets have completely merged (>500μm from the edge of the acoustic aperture, marked in blue), and a region at the edge of the lines (marked in red) where the acoustic force is weaker (corresponding to the edge of the IDTs), and droplets are still visible. Zoom in on the edge at g) t =8'30"and h) t=10'10".

can be divided in two regions: A region where almost all droplets have completely merged (>500µm from the edge of the acoustic aperture, marked in blue), and a region at the edge of the lines (marked in red) where the acoustic force is weaker, and droplets are still visible. We note that the red marked region is still within the acoustic aperture but close to the aperture's edge (see Fig. S2 in SI). This illustrates the dependence of the coalescence on the acoustic force [34]. Fig. 2g-h show the change over time at the edge. Initially (Fig. 2g), the particles are similar in size. Due to the gradient in the acoustic force, coalescence is more rapid in the upper part of the image leading to bigger droplets (Fig. 2h). Fig. S3 also shows this phenomenon for edges of three separate lines.

We note that some PDMS moieties are positioned between the patterned lines and do not move towards the nodes. This is attributed to electrostatic interactions between PDMS and the substrate that immobilizes the streaming particles before they reach the node area. Similar findings for polystyrene beads were previously reported by Wood *et al*. [27] We verified that the patterned PDMS structures are

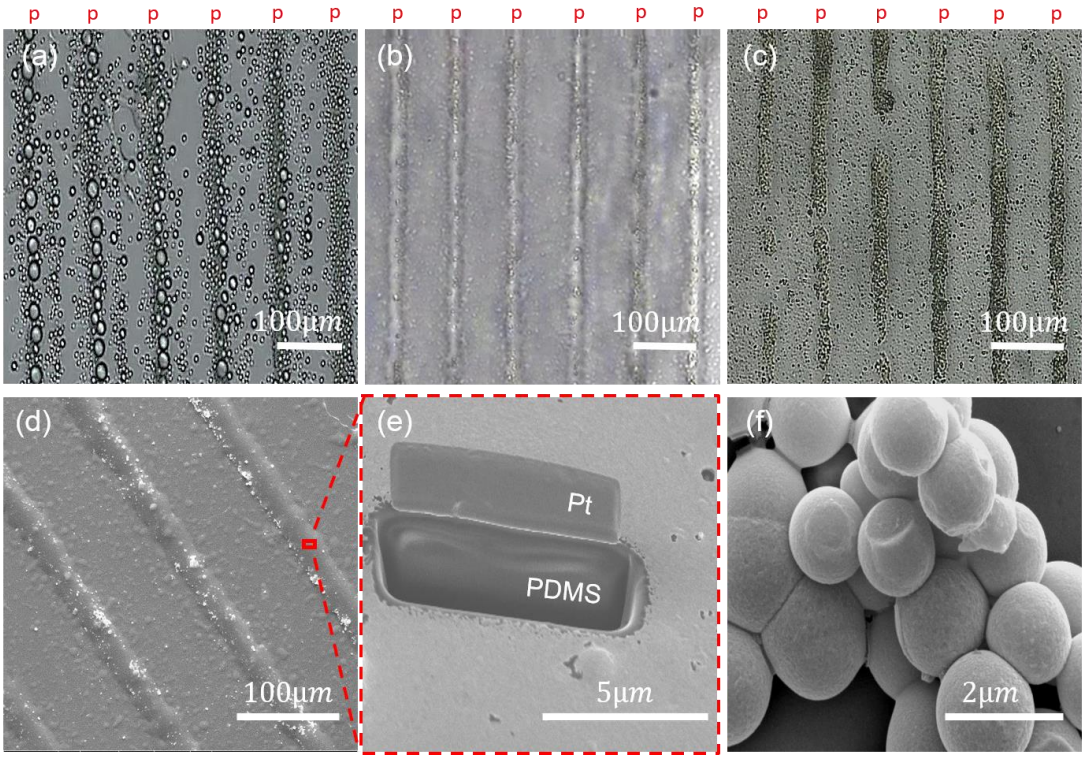

Fig. 3 Bright-field images (in situ) for different concentrations of cross-linker: a) 40% b) 80% and c) 90%. Continuous structures are only formed at 80% cross-linker. The letter "p" in red is shown above the location of the PDMS lines. d-e) SEM images of deposition from 80% cross-linker. e) A cross-section formed by FIB (Pt is used for stabilizing the surface) of part of a PDMS line (~7µm from a ~40µm wide line). The ~3µm deep trench formed by FIB show no traces of sphere like structures. f) SEM image of deposition at the nodes using 90% cross-linked PDMS.

indeed at the nodes, as silver nanoparticles that we added were also positioned in the same places (see Fig. S5 in SI). The dependence of the forming structure (1 hour after infusion) on the cross-linker ratio is shown in Fig. 3. This ratio influences the polymerization rate that plays a central role in the assembly and polymerization of the structure. Solutions with varying cross-linker concentrations were prepared and infused into the microchannel once nucleation sites started forming (at the first signs of turbidity). This correlates to 10, 10, 60, 120 minutes (±2 minutes) for 90%, 80%, 60% and 40% cross-linker ratios, respectively. At 40% (Fig. 3a) and 60% (not shown) cross-linker

ratios, the droplets wet the surface and are arranged along the nodes but do not merge to form a continuous microstructure. In these cases, in order to minimize surface tension, the coalescing particles form large separate hemispheres on the glass surface [35]. These large hemispheres collapse on drying and therefore cannot be visualized by scanning electron microscope (SEM). For 90% cross-linker amounts (Fig. 3c), particles are highly branched and cannot deform easily. As they are pushed to the nodes, they stick to the glass surface and to each other due to chemical-bond formation by the ongoing condensation reaction and hydrophobic interactions [36]. The deformation is minimal (Fig. 3f) due to their stiffness and they remain as ~1 μm micro-particles along the nodes. 80% cross-linker ratio (Fig. 3b and 3d) results in the formation of well-defined and continuous lines as previously described (Fig. 1c-e). In this case, the colliding droplets wet the glass surface along the nodes, and their high viscosity results in merging without breakup into individual hemispheres (see illustrations in Fig. 1d and 1e) thus forming well connected continuous lines (resembling continuous line formation formed by highly viscous droplets[35]). Fig. 3e shows the surface and cross-section, formed by FIB (focused ion beam), for part of an 80% cross-linked line on the glass substrate. The FIB etched only a ~3μm deep and ~7μm wide trench from a ~40μm wide line. The surface and cross-section are uniform without traces of sphere like structures or voids. This demonstrates another benefit of our method. Assembly of preformed materials would inevitably form microstructures with voids that would require a post treatment process in order to eliminate them. Here on the other hand, a void free continuous microstructure is formed in a single step. We note that if we delay (by more than 10 minutes) the infusion of the 80% cross-linked solution, we do not obtain continuous lines but rather scattered aggregates of small (~1 μm) micro-particles, as in the 90% case. This is because the rigidity of the droplets increases with time, thereby preventing deformation of the droplet.

Sodium sulfate is necessary to screen charges [37] on the PDMS nucleation sites, and its influence on the coalescence process and microstructure formation was studied. Fig. 4a-c show the SEM images of 80% crosslinked PDMS solution with 0 wt%, 0.7 wt% and 1.4 wt% sodium sulfate, respectively. In the absence of salt (Fig. 4a), the droplets do not coalesce, so that only small polymerized beads are aligned along the node line. Increasing the amount of salt to 0.7 wt% promotes coalescence and it is possible to observe the formation of continuous structures (Fig. 4b), following the mechanism stated above. If the salt concentration is further increased to 1.4 wt% (Fig. 4c), droplets coalesce rapidly and stick to the glass surface before reaching the nodes. Therefore, continuous formations are absent, and only droplet-depleted areas (the anti-nodes) can be seen.

The influence of acoustic wave intensity on width of polymerized structures (as imaged by bright-field microscopy) is shown in Fig. 5a (for 80% cross-linked PDMS with 0.7 wt% salt). Each data point is averaged for ~50 lines (8 lines each in 6 different experiments). Increasing the primary acoustic-radiation force leads to compression of nucleation sites around the pressure nodes, resulting in a decrease in width of formed lines and an increase in their maximum height (see Fig. S4 in SI). The profile of several lines assembled at 20 Vpp is demonstrated in Fig. 5b (see also Fig. S6 in SI). We note that below 12.5 Vpp we do not observe formation of continuous structures.

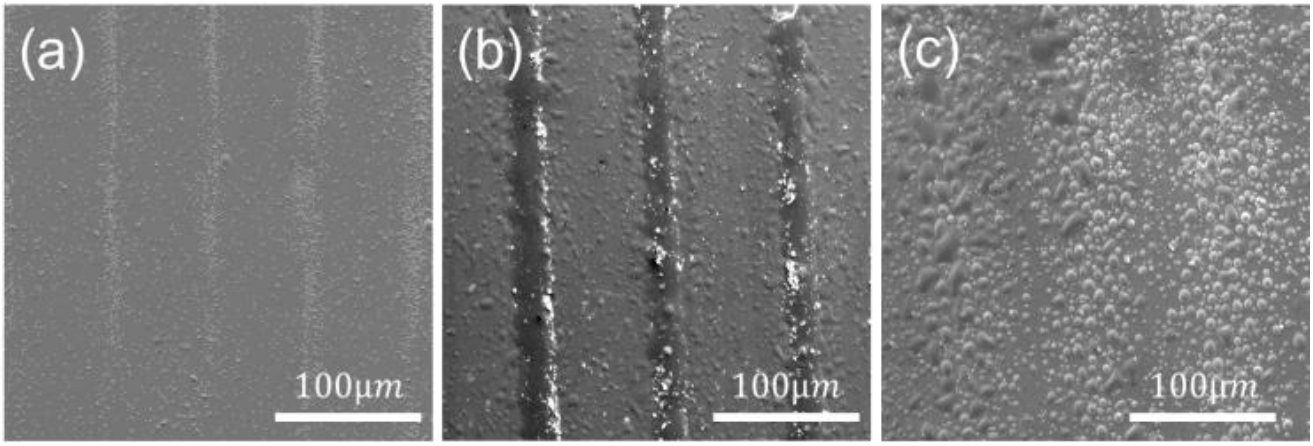

Fig. 4 SEM images at different salt concentrations. **a)** 0 wt%, **b) 0.**7 wt% and **c)** 1.4 wt% of sodium sulfate.

While here the most straightforward standing wave formation was used, future work could exploit more complex acoustic patterns based on holographic acoustics [38,39]**.** Additionally, super-high-frequency transducers could lead to significantly higher resolutions [40,41]**.** Our approach also allows directed assembly inside closed systems (such as microfluidic channels) where other assembly methods are not applicable.

Conclusions:

In conclusion, we have demonstrated directed deposition of emulsion droplets undergoing polymerization into ordered PDMS microstructures by SSAWs. This is the first realization of SSAWs being used to manipulate and spatially direct the products of an ongoing chemical reaction, rather than preformed materials. Additionally, this method provides void free polymeric microstructures without any post-processing. We have systematically studied the influence of the acoustic wave intensity, cross-linker ratio and salt concentration on the formation of the microstructures. Acoustic forces can influence almost all dispersed systems, require only low power densities and can be easily scaled up. Combining chemical synthesis with the patterning processes as shown here (a one-step procedure), can therefore be beneficial for various applications.

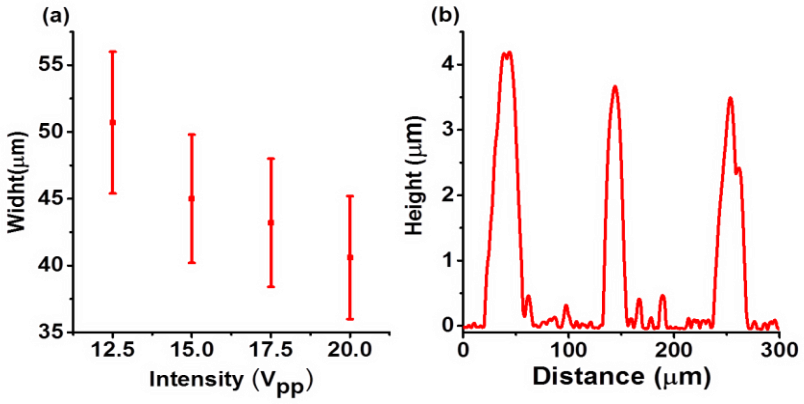

Fig. 5 a) Width of formed line structures as a function of applied RF signal. b) Profilometer measurements showing the height and width of the lines.

Acknowledgment:

We thank Bar-Ilan University for their generous start-up package.

Appendix A: Supplementary material

Supplementary data to this article can be found online at **……**

References:

[1] A. Biswas, I.S. Bayer, A.S. Biris, T. Wang, E. Dervishi, F. Faupel, Advances in top-down and bottom-up surface nanofabrication: techniques, applications & future prospects, Adv Colloid Interface Sci. 170 (2012) 2–27. doi:10.1016/j.cis.2011.11.001.
[2] N. Bhandaru, S. Roy, Suruchi, G. Harikrishnan, R. Mukherjee, Lithographic Tuning of Polymeric Thin Film Surfaces by Stress Relaxation, ACS Macro Letters. 2 (2013) 195–200. doi:10.1021/mz300577d.
[3] Y. Kumashiro, H. Nakako, M. Inada, K. Yamamoto, A. Izumi, M. Ishihara, Novel materials for electronic device fabrication using ink-jet printing technology, Applied Surface Science. 256 (2009) 1019–1022. doi:10.1016/j.apsusc.2009.05.134.
[4] N. Armon, E. Greenberg, M. Layani, Y.S. Rosen, S. Magdassi, H. Shpaisman, Continuous Nanoparticle Assembly by a Modulated Photo-Induced Microbubble for Fabrication of Micrometric Conductive Patterns, ACS Appl Mater Interfaces. 9 (2017) 44214–44221. doi:10.1021/acsami.7b14614.
[5] B. Edwards, N. Engheta, S. Evoy, Theory of simultaneous control of orientation and translational motion of nanorods using positive dielectrophoretic forces, Journal of Applied Physics. 98 (2005) 124314. doi:10.1063/1.2148627.
[6] A. Ashkin, Acceleration and Trapping of Particles by Radiation Pressure, Phys. Rev. Lett. 24 (1970) 156–159. doi:10.1103/PhysRevLett.24.156.
[7] M.C. Wu, Optoelectronic tweezers, Nat Photon. 5 (2011) 322–324. doi:10.1038/nphoton.2011.98.
[8] I.D. Vlaminck, C. Dekker, Recent Advances in Magnetic Tweezers, Annual Review of Biophysics. 41 (2012) 453–472. doi:10.1146/annurev-biophys-122311-100544.
[9] J.M. Katzenstein, D.W. Janes, J.D. Cushen, N.B. Hira, D.L. McGuffin, N.A. Prisco, C.J. Ellison, Patterning by Photochemically Directing the Marangoni Effect, ACS Macro Letters. 1 (2012) 1150–1154. doi:10.1021/mz300400p.
[10] D. Hou, H.-C. Chang, ac field enhanced protein crystallization, Appl. Phys. Lett. 92 (2008) 223902. doi:10.1063/1.2938887.
[11] J.V. Parambil, M. Schaepertoens, D.R. Williams, J.Y.Y. Heng, Effects of Oscillatory Flow on the Nucleation and Crystallization of Insulin, Crystal Growth & Design. 11 (2011) 4353–4359. doi:10.1021/cg200158z.
[12] Q.-Q. Lu, D.-C. Yin, Y.-M. Liu, X.-K. Wang, P.-F. Yang, Z.-T. Liu, P. Shang, Effect of mechanical vibration on protein crystallization, J Appl Cryst, J Appl Crystallogr. 43 (2010) 473–482. doi:10.1107/S0021889810009313.
[13] R.L. Hartman, J.P. McMullen, K.F. Jensen, Deciding Whether To Go with the Flow: Evaluating the Merits of Flow Reactors for Synthesis, Angewandte Chemie International Edition. 50 (2011) 7502–7519. doi:10.1002/anie.201004637.
[14] I. Jacob, E. Edri, E. Lasnoy, S. Piperno, H. Shpaisman, Influencing colloidal formation with optical traps, Soft Matter. 13 (2017) 706–710. doi:10.1039/C6SM02639G.
[15] A.A. Doinikov, Acoustic radiation pressure on a compressible sphere in a viscous fluid, Journal of Fluid Mechanics. 267 (1994) 1–22. doi:10.1017/S0022112094001096.
[16] X. Ding, S.-C.S. Lin, B. Kiraly, H. Yue, S. Li, I.-K. Chiang, J. Shi, S.J. Benkovic, T.J. Huang, On-chip manipulation of single microparticles, cells, and organisms using surface acoustic waves, Proceedings of the National Academy of Sciences. 109 (2012) 11105–11109.

[17] F.M. McFarland, X. Liu, S. Zhang, K. Tang, N.K. Kreis, X. Gu, S. Guo, Electric field induced assembly of macroscopic fibers of poly(3-hexylthiophene), Polymer. 151 (2018) 56–64. doi:10.1016/j.polymer.2018.07.062.
[18] G. Dominguez-Espinosa, A. Synytska, A. Drechsler, C. Gutsche, K. Kegler, P. Uhlmann, M. Stamm, F. Kremer, Optical tweezers to measure the interaction between poly(acrylic acid) brushes, Polymer. 49 (2008) 4802–4807. doi:10.1016/j.polymer.2008.09.007.
[19] J. Shi, H. Huang, Z. Stratton, Y. Huang, T.J. Huang, Continuous particle separation in a microfluidic channelvia standing surface acoustic waves (SSAW), Lab Chip. 9 (2009) 3354–3359. doi:10.1039/B915113C.
[20] F. Guo, Z. Mao, Y. Chen, Z. Xie, J.P. Lata, P. Li, L. Ren, J. Liu, J. Yang, M. Dao, S. Suresh, T.J. Huang, Three-dimensional manipulation of single cells using surface acoustic waves, Proc. Natl. Acad. Sci. U.S.A. 113 (2016) 1522–1527. doi:10.1073/pnas.1524813113.
[21] F. Guo, P. Li, J.B. French, Z. Mao, H. Zhao, S. Li, N. Nama, J.R. Fick, S.J. Benkovic, T.J. Huang, Controlling cell-cell interactions using surface acoustic waves, Proc. Natl. Acad. Sci. U.S.A. 112 (2015) 43–48. doi:10.1073/pnas.1422068112.
[22] Y. Chen, S. Li, Y. Gu, P. Li, X. Ding, L. Wang, J.P. McCoy, S.J. Levine, T.J. Huang, Continuous enrichment of low-abundance cell samples using standing surface acoustic waves (SSAW), Lab Chip. 14 (2014) 924–930. doi:10.1039/C3LC51001H.
[23] F. Guo, W. Zhou, P. Li, Z. Mao, N.H. Yennawar, J.B. French, T.J. Huang, Precise Manipulation and Patterning of Protein Crystals for Macromolecular Crystallography Using Surface Acoustic Waves, Small. 11 (2015) 2733–2737. doi:10.1002/smll.201403262.
[24] M. Sesen, T. Alan, A. Neild, Microfluidic on-demand droplet merging using surface acoustic waves, Lab Chip. 14 (2014) 3325–3333. doi:10.1039/c4lc00456f.
[25] M.K. Nichols, R.K. Kumar, P.G. Bassindale, L. Tian, A.C. Barnes, B.W. Drinkwater, A.J. Patil, S. Mann, Fabrication of Micropatterned Dipeptide Hydrogels by Acoustic Trapping of Stimulus-Responsive Coacervate Droplets, Small. 14 (2018) e1800739. doi:10.1002/smll.201800739.
[26] S. Wollmann, R.B. Patel, A. Wixforth, H.J. Krenner, Ultrasonically assisted deposition of colloidal crystals, Applied Physics Letters. 105 (2014) 031113.
[27] C.D. Wood, S.D. Evans, J.E. Cunningham, R. O'Rorke, C. Wälti, A.G. Davies, Alignment of particles in microfluidic systems using standing surface acoustic waves, Applied Physics Letters. 92 (2008) 044104. doi:10.1063/1.2838748.
[28] H. Sazan, S. Piperno, M. Layani, S. Magdassi, H. Shpaisman, Directed Assembly of Nanoparticles into Continuous Microstructures by Standing Surface Acoustic Waves, Journal of Colloid and Interface Science. 536 (2019) 701–709. doi:10.1016/j.jcis.2018.10.100.
[29] T.M. Obey, B. Vincent, Novel monodisperse 'silicone oil'/water emsulsions, J.Colloid Interface Sci. 163 (1994). http://research-information.bristol.ac.uk/en/publications/novel-monodisperse-silicone-oilwater-emsulsions(86defeff-2dc0-480c-ac22-6170a8ab5145)/export.html (accessed August 17, 2016).
[30] G. Gillies, C.A. Prestidge, P. Attard, An AFM Study of the Deformation and Nanorheology of Cross-Linked PDMS Droplets, Langmuir. 18 (2002) 1674–1679. doi:10.1021/la011461g.
[31] A. Rahimi, P. Shokrolahi, Application of inorganic polymeric materials: I. Polysiloxanes, International Journal of Inorganic Materials. 3 (2001) 843–847. doi:10.1016/S1466-6049(01)00162-3.
[32] C. Wang, H. Shpaisman, A.D. Hollingsworth, D.G. Grier, Celebrating Soft Matter's 10th Anniversary: Monitoring colloidal growth with holographic microscopy, Soft Matter. 11 (2015) 1062–1066. doi:10.1039/C4SM01979B.
[33] F. Guo, Y. Xie, S. Li, J. Lata, L. Ren, Z. Mao, B. Ren, M. Wu, A. Ozcelik, T.J. Huang, Reusable acoustic tweezers for disposable devices, Lab Chip. 15 (2015) 4517–4523. doi:10.1039/c5lc01049g.
[34] W. Xie, R. Li, X. Lu, P. Han, S. Gu, Acoustically aided coalescence of water droplets and dehydration of crude oil emulsion, Korean J. Chem. Eng. 32 (2015) 643–649. doi:10.1007/s11814-014-0253-6.
[35] M.W. Lee, N.Y. Kim, S. Chandra, S.S. Yoon, Coalescence of sessile droplets of varying viscosities for line printing, International Journal of Multiphase Flow. 56 (2013) 138–148. doi:10.1016/j.ijmultiphaseflow.2013.06.004.
[36] M. Ichikawa, Y. Matsuzawa, Y. Koyama, K. Yoshikawa, Molecular Fabrication: Aligning DNA Molecules as Building Blocks, Langmuir. 19 (2003) 5444–5447. doi:10.1021/la034338t.
[37] B. Neumann, B. Vincent, R. Krustev, H.-J. Müller, Stability of Various Silicone Oil/Water Emulsion Films as a Function of Surfactant and Salt Concentration, Langmuir. 20 (2004) 4336–4344. doi:10.1021/la035517d.
[38] A.L. Bernassau, C. K. Ong, Y. Ma, P.G.A. Macpherson, C.R.P. Courtney, M. Riehle, B.W. Drinkwater, D.R.S. Cumming, Two-dimensional manipulation of micro particles by acoustic radiation pressure in a heptagon cell, IEEE Transactions on Ultrasonics, Ferroelectrics and Frequency Control. 58 (2011) 2132–2138. doi:10.1109/TUFFC.2011.2062.
[39] K. Melde, A.G. Mark, T. Qiu, P. Fischer, Holograms for acoustics, Nature. 537 (2016) 518–522. doi:10.1038/nature19755.
[40] A.B.A. Dow, C. Popov, U. Schmid, N.P. Kherani, Super-high-frequency SAW transducer utilizing AIN/ultrananocrystalline diamond architectures, IEEE Transactions on Ultrasonics, Ferroelectrics, and Frequency Control. 60 (2013) 1581–1586. doi:10.1109/TUFFC.2013.2738.
[41] D.J. Collins, A. Neild, Y. Ai, Highly focused high-frequency travelling surface acoustic waves (SAW) for rapid single-particle sorting, Lab on a Chip. 16 (2016) 471–479. doi:10.1039/C5LC01335F.

Supplementary Information

Simultaneous Polymerization and Patterning: A One Step Acoustic Directed Assembly Method

*Silvia Piperno, Haim Sazan and Hagay Shpaisman**

Department of Chemistry, Institute for Nanotechnology and Advanced Materials,

Bar Ilan University, Ramat Gan, 5290002, Israel

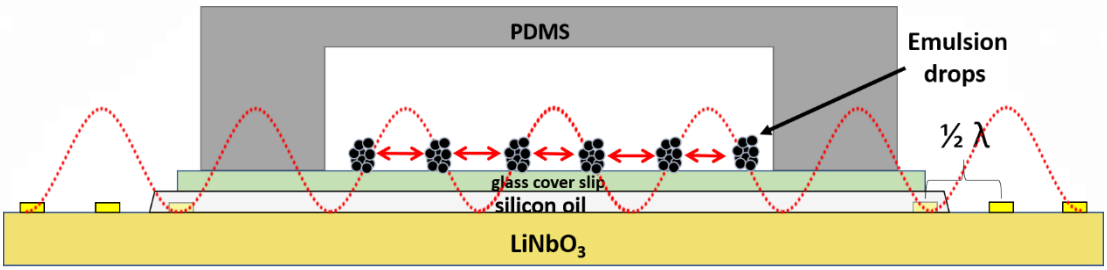

Figure.S1 Cross-section (not to scale) of the experimental system showing the primary acoustic force (red arrows) that drives the NPs towards the pressure nodes of the SSAWs. A cover slip is bonded to the PDMS channel and positioned between the two IDTs. Silicon oil is used to acoustically couple the glass substrate to the lithium niobate.

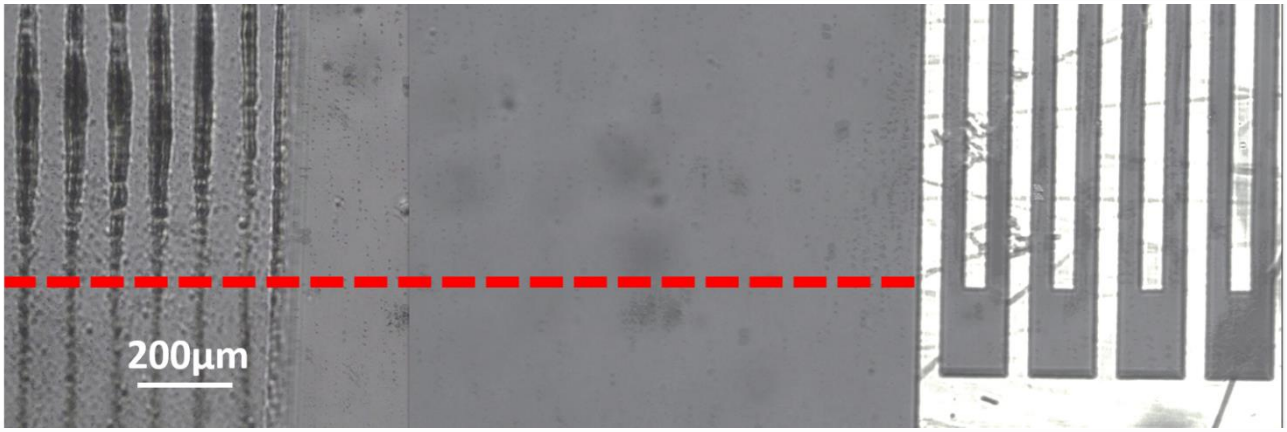

Figure. S2 Bright field microscopy image (formed by image stitching) showing the position of the IDTs relative to the pattern formation. The red dashed line represents the edge of the overlapping electrodes (the area that generates the acoustic wave).

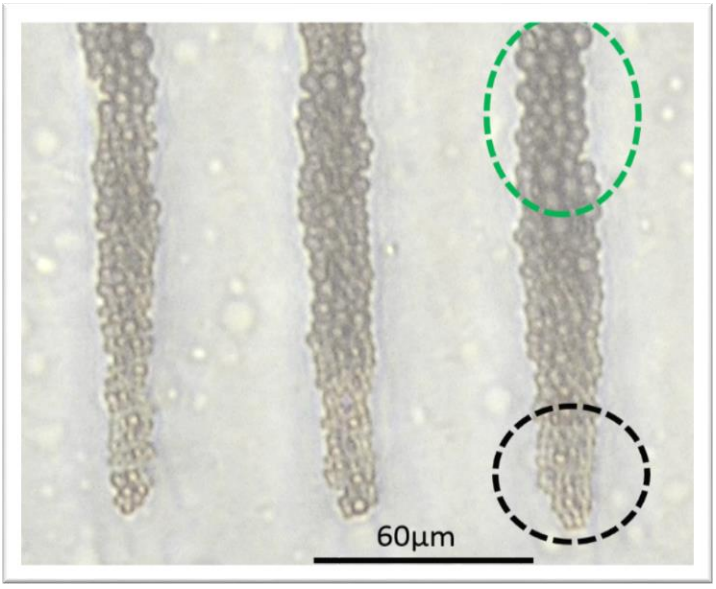

Figure. S3 Bright field microscopy images of the edge of the lines formed by SSAWs. Gradient of the acoustic force along the acoustic nodes leads to presence of bigger drops in the upper part of the image (green dashed line) where the coalescence is favored (stronger primary acoustic force) compared to the lower part (black dashed line) where the primary acoustic force is weaker.

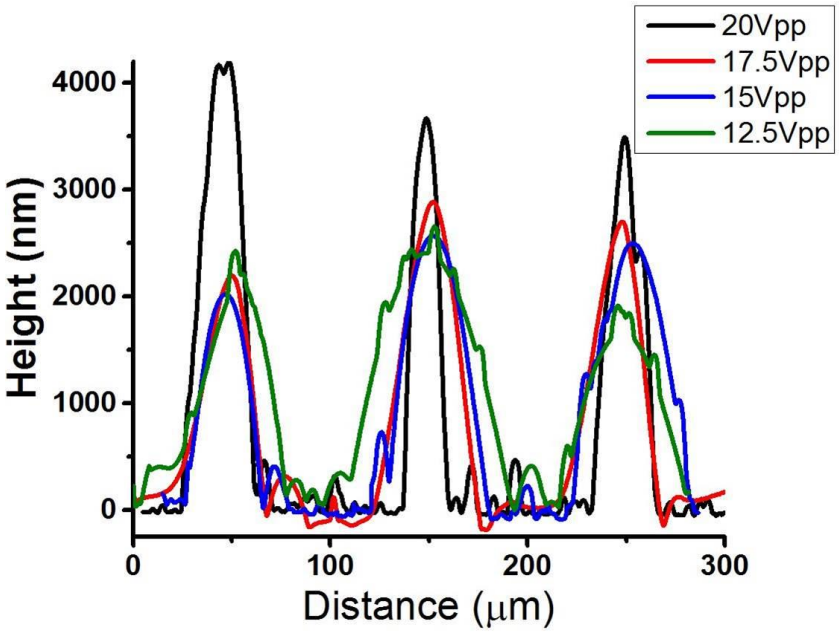

Figure. S4 Profilometer measurements showing the height and width of the lines for various applied voltages. All measurements were performed on polymerized samples (after washing with water and drying).

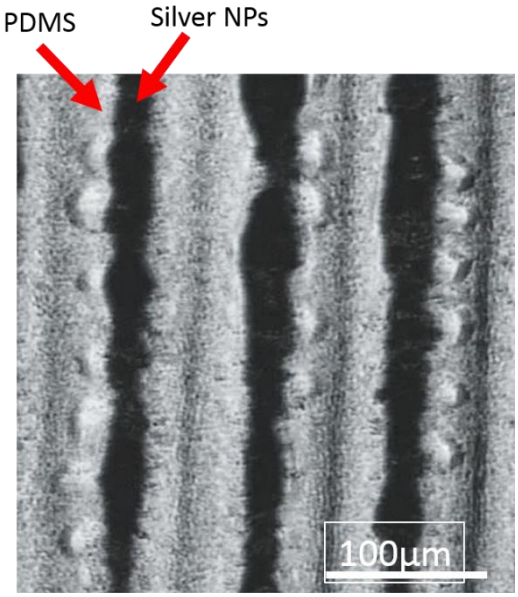

Figure. S5 Bright-field microscopy image of a mixture of PDMS droplets and AG NPs under SSAWs showing that both are attracted to the same location (pressure nodes).

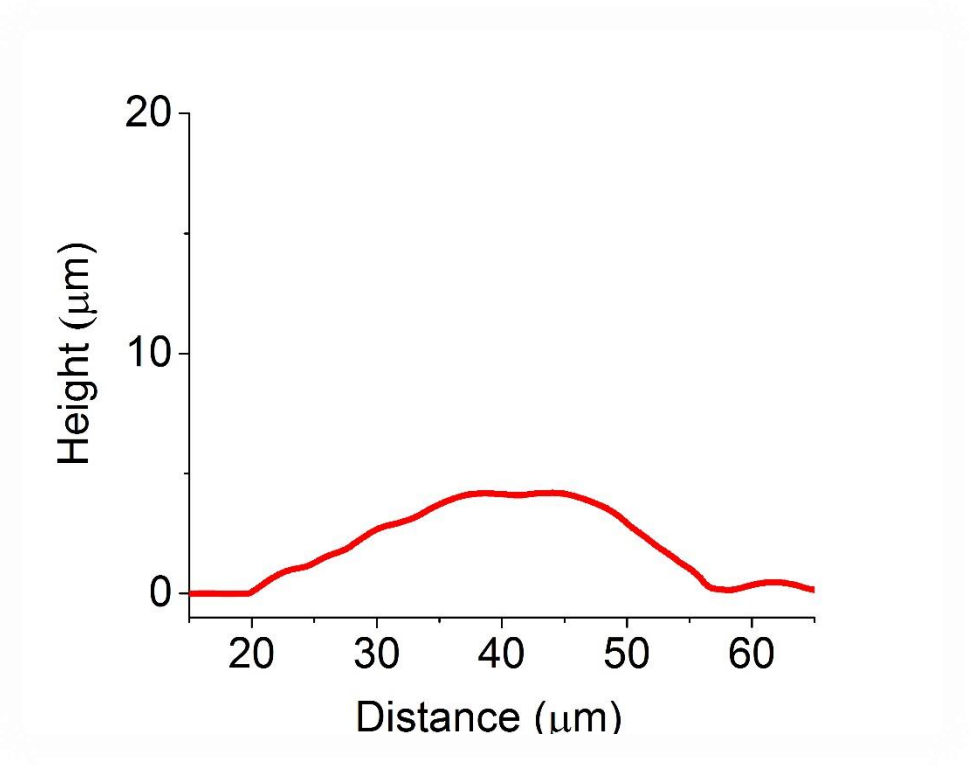

Figure. S6 Profilometer measurements of a single line (replot of Figure 5b). The hemispherical characteristic is clearly visible.

Acoustic contrast factor calculation

The continuous phase in the studied system is a solution of water, ammonium solution and Na_2SO_4. The measured density of the medium is therefore 0.983 gr/ml. Using the range of bulk moduli previously reported for PDMS (2.2-4.95GPa, Johnston et al. J. Micromech. Microeng 24 (2014) 035017), our calculated acoustic contrast factor is positive, ranging between 0.02 to 0.55. We have also observed experimentally that PDMS in our solution indeed act as particles with a positive acoustic contrast factor (attracted to pressure nodes). A PDMS emulsion (80% cross-linker) was infused in the PDMS micro-channel and directed by applying the SSAWs. After 9 minutes, silver nanoparticles (NPs, synthesized as described by Magdassi et al. ACS Nano 2010, 4, 1943−1948) were infused into the micro-channel. The Silver NPs (that have a positive contrast acoustic factor) were driven by the SSAWs to the same locations (pressure nodes) as the previously deposited PDMS (Figure S5).

Acoustic force calculation

The acoustic force applied on 1 μm diameter emulsion droplets of PDMS (80% cross-linked in a 0.7 wt% solution of $NaSO_4$) was calculated for spheres in proximity (<10μm) to the pressure antinodes (where the acoustic field is maximal). This was determined by tracking their motion immediately after turning on the acoustic field generated by applying 20Vpp at F=19.4Mhz on the IDTs. The velocity of the spheres after 0.1 seconds was 61±11μm/sec. The acoustic force can be expressed as

$F_{acoustic} = F_{observed} + F_{drag}$

Where

$F_{drag}=6\pi\eta r v$

Where η, r and v represent the viscosity of the surrounding medium, radius of the particle and velocity of the particles, respectively. Using this approximation, the acoustic force under these conditions was found to be $\cong 3.3*10^{-13}$N.

SV1 Video showing nucleation sites moving to pressure nodes as the acoustic waves are turned on. Sample of 80% cross-linker. The solution was infused into the PDMS micro-channel ~10 min after preparation.

SV2 Video showing big droplets (infused to the PDMS micro-channel ~40min after preparation) moving to pressure nodes as the acoustic waves are turned on. The only purpose of this video is to allow tracking of individual particles (not used for formation of continuous lines).

SV3 Video showing the coalescence and wetting process in the presence of acoustic waves (80% cross-linker).

SV4 Video of PDMS colloids (80% cross-linker) without applying acoustic waves. The solution was infused to the PDMS micro-channel ~15min after preparation.